OPTICAL FLOW METHOD IN PHASE-CONTRAST MICROSCOPY IMAGES FOR THE DIAGNOSIS OF PRIMARY CILIARY DYSKINESIA THROUGH MEASUREMENT OF CILIARY BEAT FREQUENCY. PRELIMINARY RESULTS.

Eduardo Parrilla[1], Miguel Armengot[2], Manuel Mata[3], Julio Cortijo[3], Jaime Riera[4], José L. Hueso[4], David Moratal[5]

[1]Biomechanics Institute of Valencia, Valencia, Spain
[2]Primary Ciliary Dysquinesia Unit of the General and University Hospital, Valencia University, Spain
[3]Researh Department, General and University Hospital, Valencia University, Spain
[4]Institute of Multidisciplinary Mathematics, Universitat Politècnica de València, Valencia, Spain
[5]Center for Biomaterials and Tissue Engineering, Universitat Politècnica de València, Valencia, Spain

ABSTRACT

Primary ciliary dyskinesia (PCD) implies cilia with dysmotility or total absence of motility, which may result in sinusitis, chronicbronchitis, bronchiectasis and male infertility. A large number of deficiencies detectable on the ultrastructural level give rise to PCD, but patients with normal cilia ultrastructure are common. An early diagnosis is very important since PCD can cause permanent lung damage. Diagnosis can be difficult and is based on an abnormal ciliary beat frequency (CBF) and beat pattern, accompanied by specific abnormalities of the ciliary axoneme or normal ultrastructural cilia. In this paper, we present a method to determine CBF through the analysis of phase-contrast microscopy imaging acquired using digital high speed video techniques. Beat frequency measurements are made estimating cilia motion by means of an optical flow algorithm. A previous coregistration process is performed to eliminate cell movements due to cilia motion. The algorithm is tested on several isolated ciliar cells, concluding that this method is a robust technique to determine CBF.

Index Terms— Active contours, beat frequency, Fourier-Mellin transform, optical flow

1. INTRODUCTION

Primary ciliary dyskinesia (PCD) is an autosomal recessive inherited disorder affecting approximately 1:10,000 to 1:30,000 individuals [1-3]. It causes a defect in the action of the cilia lining the respiratory tract, Fallopian tube and spermatozoid flagella. PCD is characterized by the complete absence of mucociliary clearance, leading to respiratory symptoms and signs typically present since birth and predisposing affected individuals to recurrent respiratory infections [4]. Despite persistent symptoms, and often attendance at ear, nose, and throat and respiratory clinics, many patients with PCD are not diagnosed until later in life [5], by which time permanent lung damage has occurred [6]. Early and accurate diagnosis is important, because once made, lung function can be maintained with specialist respiratory care [7-9]. The diagnosis of PCD is traditionally made on the basis of a supportive clinical history and an abnormal ciliary beat frequency (CBF).

A commonly used method to estimate CBF using a digital high speed video analysis (DHSV) has been explained in [10, 11]. This method computes the Fast Fourier Transform (FFT) of the intensity signals in a window of 3×3 pixels centered on a selected pixel above the cilium. This technique does not consider the global movement of all cilia and local illumination changes can affect the results. On the other hand, this method is not valid when the cell is moving due to its own ciliar beat.

In this paper, we present a method to measure CBF of isolated cells based on the analysis of the cilia global movement by means of optical flow algorithms. A coregistration process is also implemented to eliminate the cell movement effects.

2. METHOD

2.1. Image Acquisition

Ciliar cells were mounted onto the stage of a Nikon Eclipse TE100 microscope, by using a 40x Nikon lens with a final optical gain of 400x. The microscope was connected to a CCD camera (Digital Quad High Speed Progressive Scan Camera, JAI CV-A33 CL) that records images with a matrix size of 649x494 pixels, and a rate of 120 frames per second. Images were acquired into a HP Workstation xw6200 Xeon 3.4 GHz with 2Gb of RAM system by means of an image

acquisition board (NI PCIe-1429, Full Configuration Camera Link Image Acquisition).

2.2. Coregistration

Ciliated samples are placed in a liquid solution. Therefore, ciliar beat can cause a movement of the cells to analyze. In general, there are two groups: isolated cells that have a rotation movement, and cells that are sticked on other components of the solution and keep still. In the first case, it is necessary to eliminate this rotation movement to estimate CBF.

2.2.1. Cell segmentation

For initiating the coregistration process, it is necessary to localize the cell to analyze. We propose an automatic segmentation method based on gradient vector flow snakes to perform this task. A snake is an energy-minimizing spline guided by external constraint forces and influenced by image forces that pull it toward features such as lines and edges [12]. Instead of exploiting only image information as low-level edge-detection techniques do, snakes also use information about the boundaries as part of an optimization procedure. Snakes are active contour models: they lock onto nearby edges, localizing them accurately.

The active-contour model involves vertices connected by edge segments with, in general, two associated force terms. The internal force is computed based on the local shape of the contour. The external force (or image force) that drives the active contour to the boundary can be based on any conventional edge-detection technique. The internal and external forces may be weighted differently.

Mathematically, a snake can be defined in discrete form as a curve $\mathbf{x}(s) = [x(s), y(s)]$, $s \in [0, 1]$ that moves through the spatial domain of an image to minimize the energy functional

$$E = \int_0^1 \frac{1}{2}(\alpha \left|\mathbf{x}'(s)\right|^2 + \beta \left|\mathbf{x}''(s)\right|^2) + E_{ext}(\mathbf{x}(s))ds \qquad (1)$$

where α and β are weighting parameters that control the active contour's tension and rigidity respectively, and govern the effect of the derivatives of $\mathbf{x}(s)$. The external energy function E_{ext} is derived from the image so that it takes on its smaller values at the features of interest such as boundaries.

A snake that minimizes (1) must satisfy the Euler equation

$$\alpha \mathbf{x}''(s) - \beta \mathbf{x}''''(s) - \nabla E_{ext} = 0 \qquad (2)$$

where $F_{\text{int}} = \alpha \mathbf{x}''(s) - \beta \mathbf{x}''''(s)$ and $F_{ext} = -\nabla E_{ext}$ comprise the components of a force balance equation such that $F_{\text{int}} + F_{ext} = 0$.

Xu and Prince [13] proposed Gradient Vector Flow (GVF) to improve the capture range of the image force. GVF involves a vector field derived by solving a vector diffusion equation which diffuses the gradient vectors of a grey-level image. The solution for the GVF vector field involves a combination of Laplacian and gradient terms, and a blending factor is used for governing the trade-off between them. GVF snakes replace the potential force $-\nabla E_{ext}$ by the gradient vector flow field.

In our method, the segmentation of the first frame is used as a first contour estimation of the other sequence frames. Using this initial estimation, the algorithm computes an iterative process to perform the cell segmentation in each frame.

2.2.2. Rotation Correction

Segmented images are used to center the cell in the middle of the images. In this way, the centroid of the segmented region is situated in the center of the image. This point is considered as the rotation axis. Once the cell is centered, for each frame, the rotation is corrected by using a method based on Fourier-Mellin transforms [14]. The solution of this problem consists in finding the angle that each frame forms with the first frame of the sequence.

We consider a function of two variables in polar coordinates $f(r,\theta), \forall (r,\theta) \in R_+^* \cdot S^1$ where r is the radial variable and θ is the angular variable. For this function, the Analytic Fourier-Mellin Transform (AFMT) is defined as [15]

$$M_{f_\sigma}(k,v) = \frac{1}{2\pi}\int_0^\infty \int_0^{2\pi} f(r,\theta) r^{\sigma - iv} e^{-ik\theta} d\theta \frac{dr}{r} \qquad (3)$$

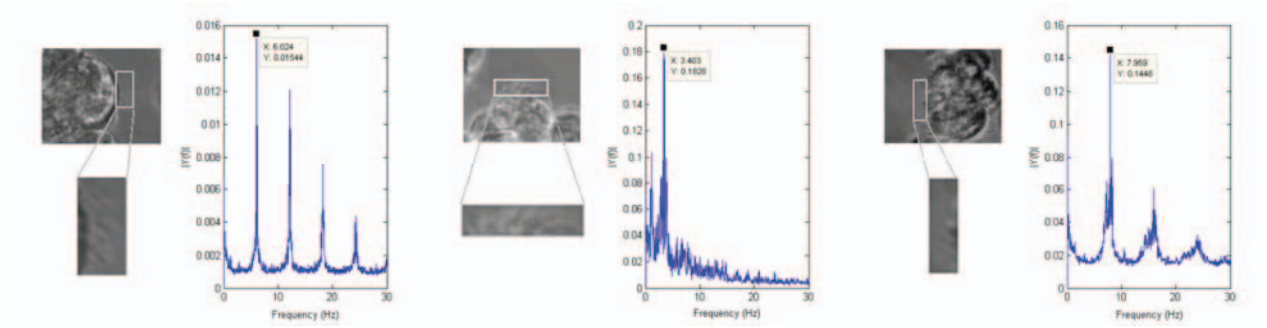
where σ is a positive constant that prevents the divergence when $r \to 0$. We can define the following function

$$E_{f,g}(\rho,\varphi) = \left(\int_0^\infty \int_0^{2\pi} r^{2\sigma} \left| f(r,\theta) - g(\rho r, \theta + \varphi) \right|^2 d\theta \frac{dr}{r} \right)^{\frac{1}{2}} \qquad (4)$$

This function measures, in all points of parameter space (ρ,φ), the similarity between both functions. It can be demonstrated that, for $\rho = 1$, (4) is equivalent to

$$E_{f,g}(\varphi) = \left(\int_{-\infty}^{+\infty} \sum_{k \in Z} \left| M_{f_\sigma}(k,v) - e^{ik\varphi} M_{g_\sigma}(k,v) \right|^2 dv \right)^{\frac{1}{2}} \qquad (5)$$

If $f(r,\theta)$ denotes the intensity function of an image and $g(r,\theta)$ is the intensity function of the same image but rotated, the angle φ_m that minimizes (5) is the angle that both images form.



(a) (b) (c)

Figure 1. Frequency analysis results of the CBF calculation for three different cases.

An advantage of this method is that the calculation of the AFMT is very fast because, with a change of variables, it can be converted in a FFT.

2.3. Measurement of CBF

Once the movement of the cell has been eliminated, a region of interest (ROI) is selected. This ROI includes all cilia and their movement along all the sequence. For the CBF analysis, a motion estimation technique based on optical flow has been implemented.

For computing the optical flow of a frame of a video sequence, it is necessary to assume that intensity variations of the image are only caused by displacements of the objects, without considering other causes such as changes of illumination. This hypothesis, proposed initially by Horn and Schunck [16], supposes that present intensity structures in the image, at local level, stay constant throughout the time, at least during small temporal intervals. Optical flow equation is defined as

$$I_x u + I_y v + I_t = 0 \tag{6}$$

where I_x, I_y are the components of the spatial gradient, I_t denotes partial differentiation with respect to time and $\mathbf{v}=(u,v)$ denotes the components of the image velocity field. The distribution of the velocity in each point of the image is known as the optical flow. Constraint (6) is not sufficient to solve the optical flow equation for a given frame. Proesmans et al. [17] present a method similar to that of Horn and Schunck. The main differences are that a matching process is incorporated into the constraint equation and a method for dealing with discontinuous flows is introduced. This approach is basically a merger of correlation and differential techniques. The proposed algorithm computes optical flow using a coupled set of non linear equations

$$\begin{aligned} \frac{\partial u}{\partial t} &= \nabla^2 u - \lambda I_x (I_x u + I_y v + I_t(\tilde{u},\tilde{v})) \\ \frac{\partial v}{\partial t} &= \nabla^2 v - \lambda I_y (I_x u + I_y v + I_t(\tilde{u},\tilde{v})) \end{aligned} \tag{7}$$

where $(\tilde{u},\tilde{v})$ can be any estimate of the velocity components and λ is a parameter which controls the balancing between image matching and flow field smoothness. The solution of (7) consists in an iterative process where $(\tilde{u},\tilde{v})$ are chosen to be the estimates of the previous iteration.

Optical flow computation produces an individual displacement signal $d_i(t)$ for each pixel i along time. The approach used to estimate CBF computes the sum of the FFT of these signals

$$Y(f) = \frac{1}{NL}\sum_{i=1}^{N} \left| FFT\left(d_i(t)\right) \right| \tag{8}$$

where N is the number of signals or number of pixels in the ROI and L is the length of the signals or number of analyzed frames.

3. RESULTS

In this section, we present experiments that apply the exposed technique to images from real ciliar cells. Our method has been tested on three phase-contrast microscopy image sequences. In all examples, for the optical flow calculation, the smoothness constraint, λ, has been set to 40, and a number of fifteen relaxation iterations has been selected.

In Fig. 1.a, we can observe the CBF calculation for a cell. In this case, the CBF value is 6.02Hz. We can see other frequency components that correspond to harmonics of the fundamental frequency. Cilia of normal cells are characterized by a whip-like movement that corresponds to

a sawtooth displacement signal and its spectrum contains both even and odd harmonics of the fundamental frequency.

In the case of cell in Fig. 1.b, analyzing the sum of the FFTs, we obtain a CBF value of 3.4Hz. In this sequence, a high noise level is present and harmonics are not visible. This defect can be due to the image acquisition process. Despite that all video sequences have been acquired with the same system, microscope focusing and illumination control is a manual process that can cause small defects in the different acquisitions. Perhaps, an improvement of this process must be developed in order to homogenize image acquisition.

The computed CBF for cell in Fig.1.c value is 7.96Hz. In this case, noise level is low and we can observe the harmonics of the fundamental frequency.

All examples have also been analyzed using the method described in [10, 11], obtaining similar results (6Hz, 3.45Hz and 7.9Hz respectively for cells in Fig. 1). These results verify the correct performance of our method.

4. CONCLUSION

Recently, new high-resolution digital high speed video (DHSV) imaging has allowed the precise beat pattern to be viewed in different planes in slow motion or frame by frame improving the traditional methods for CBF measurement (modified photodiode or photomultiplier methods). However, the DHSV technique remains imperfect and may realize erroneous measures, especially in the context of in situ measures of CBF from biopsies.

In this work, we analyze cilia motion with a novel technique based on optical flow. Compared to existing approaches in this field, our approach is a substantial improvement for studying the cilia movement. Conventional methods, which analyze the intensity variations of an isolated pixel, are not robust to noise and illumination changes due to the own cilia movement. These methods estimate CBF using local information. On the other hand, our method estimates CBF extracting the movement of all pixels that belong to cilia. This global information can also be used to obtain a complete pattern of movement and detect other possible anomalies in the movement and characteristics of cilia.

This study provides an important improvement of the DHSV technique, which allows performing CBF measures directly from biopsies of the suspected PCD patients in no more that 30 minutes without external altering factors. This fact permits an easy and immediate diagnosis of ciliary activity in situ avoiding complications and large time processing samples presents in other diagnostic tools.

5. ACKNOWLEDGEMENTS

The support of the *Vicerectorado de Investigación* of the *Universitat Politècnica de València* through project "*Proyectos de Nuevas Líneas de Investigación Multidisciplinares*" PAID-05-10 / 2697 and *Ministerio de Ciencia e Innovación* of Spain MTM2010-18539 are acknowledged.

6. REFERENCES

[1] B. A. Afzelius, "A human syndrome caused by immotile cilia," *Science*, vol. 193, no. 4250, pp. 317-319, 1976.
[2] B. A. Afzelius, "The immotile-cilia syndrome and other ciliary diseases," *Int Rev Exp Pathol*, vol. 19, pp. 1-43, 1979.
[3] B. A. Afzelius, "Immotile cilia syndrome: past, present, and prospects for the future," *Thorax*, vol. 53, pp. 894-897, 1998.
[4] M. Armengot et al., "Discinesia ciliar primaria. Ciliopatías," *Acta Otorrinolaringol Esp*., vol. 61, no. 2, pp.149-159, 2010.
[5] J. A. Turner, C. W. Corkey, J. Y. Lee, H. Levison, J. Surgess, "Clinical expression of immotile cilia syndrome," *Pediatrics*, vol. 67, pp. 805-810, 1981.
[6] A. Ellerman, H. Bisgaard, "Longitudinal study of lung function in a cohort of primary ciliary dyskinesia," *Eur Resp J*, vol. 10, pp. 2376-2379, 1997.
[7] C. W. Corkey, H. Levison, J. A. P. Turner, "The immotile cilia syndrome. A longitudinal survey," *Am Rev Respir Dis*, vol. 124, pp. 544-589, 1981.
[8] M. A. Greenstone, P. Stanley, P. Cole, I. Mackay, "Upper airway manifestations of primary ciliary dyskinesia," *J Laryngol Otol*, vol. 99, pp. 985-991, 1985.
[9] P. J. Hadfield, J. M. Rowes-Jones, A. Bush, I. Mackay, "Treatment of otitis media with effusion in children with primary ciliary dyskinesia," *Clin Otolaryngol*, vol. 22, pp. 302-306, 1997.
[10] M. Salathe, R. J. Bookman, "Mode of Ca2+ action on ciliary beat frequency in single ovine airway epithelial cells," *J Physiol*, vol. 520, no. 3, pp. 851-865, 1999.
[11] Z. Sutto, G. E. Conner, M. Salathe, "Regulation of human airway ciliary beat frequency by intracellular pH," *J Physiol*, vol. 560, no. 2, pp. 519-532, 2004.
[12] M. Kass, A. Witkin, D.Terzopoulos, "Snakes: Active contour models," *Int. J. Computer Vision*, vol. 1, no. 4, pp. 321-331, 1987.
[13] C. Xu, J. L. Prince, "Gradient vector flow: a new external force for snakes," *IEEE Conference Proceedings on Computer Vision and Pattern Recognition*, pp. 66-71, 1997.
[14] R. Courant, D. Hilbert, "Methods of Mathematical Physics," *Interscience*, NewYork, vol. 1, 1953.
[15] S. Derrode "Représentation de formes planes à niveaux de gris par différentes approximations de Fourier-Mellin analytique en vue d'indexation de bases d'images," Ph.D. dissertation, ENST-Bretagne, 1999.
[16] B. K. P. Horn, B. G. Schunck, "Determining optical flow," *Artificial Intelligence*, vol. 17, no. 1-3, pp. 185-203, 1981.
[17] M. Proesmans, L. Van Gool, E. Pauwels, A. Oosterlinck, "Determination of optical flow and its discontinuities using non-linear diffusion," in *3rd Eurpoean Conference on Computer Vision, ECCV'94*, vol. 2, pp. 295-304, 1994.